processes

MDPI

Article

Hybrid CNC–MXene Nanolubricant for Tribological Application: Characterization, Prediction, and Optimization of Thermophysical Properties Evaluation

Sakinah Muhamad Hisham [1,*], Norazlianie Sazali [1,2,*], Kumaran Kadirgama [3,4,5], Devarajan Ramasamy [3,4], Mohd Kamal Kamarulzaman [6], Lingenthiran Samylingam [7], Navid Aslfattahi [8] and Chee Kuang Kok [7]

1 Faculty of Manufacturing and Mechatronic Engineering Technology, University Malaysia Pahang Al Sultan Abdullah, Pekan 26600, Malaysia
2 Center of Excellence for Advanced Research in Fluid Flow, Universiti Malaysia Pahang Al Sultan Abdullah, Pekan 26600, Malaysia
3 Advanced Nano Coolant-Lubricant (ANCL) Lab, Automotive Engineering Centre, Universiti Malaysia Pahang Al Sultan Abdullah, Pekan 26600, Malaysia; kumaran@umpsa.edu.my (K.K.); deva@umpsa.edu.my (D.R.)
4 Faculty of Mechanical and Automotive Engineering Technology, Universiti Malaysia Pahang Al Sultan Abdullah, Pekan 26600, Malaysia
5 Department of Civil Engineering, College of Engineering, Almaaqal University, Basra 61003, Iraq
6 Faculty of Engineering, Universiti Malaysia Sabah, Jalan UMS, Kota Kinabalu 88400, Malaysia; mohd.kamal@ums.edu.my
7 Centre for Advanced Mechanical and Green Technology, Faculty of Engineering and Technology, Multimedia University, Jalan Ayer Keroh Lama, Bukit Beruang, Melaka 75450, Malaysia; lingenthiran@mmu.edu.my (L.S.); ckkok@mmu.edu.my (C.K.K.)
8 Institute of Fluid Mechanics and Thermodynamics, Faculty of Mechanical Engineering, Czech Technical University in Prague, Technická 4, 166 07 Prague, Czech Republic; navid.aslfattahi@fs.cvut.cz
* Correspondence: sakinahmh@umpsa.edu.my (S.M.H.); azlianie@umpsa.edu.my (N.S.)

Citation: Hisham, S.M.; Sazali, N.; Kadirgama, K.; Ramasamy, D.; Kamarulzaman, M.K.; Samylingam, L.; Aslfattahi, N.; Kok, C.K. Hybrid CNC–MXene Nanolubricant for Tribological Application: Characterization, Prediction, and Optimization of Thermophysical Properties Evaluation. *Processes* **2024**, *12*, 2146. https://doi.org/10.3390/pr12102146

Academic Editor: Blaž Likozar

Received: 28 August 2024
Revised: 19 September 2024
Accepted: 24 September 2024
Published: 2 October 2024

Copyright: © 2024 by the authors. Licensee MDPI, Basel, Switzerland. This article is an open access article distributed under the terms and conditions of the Creative Commons Attribution (CC BY) license (https://creativecommons.org/licenses/by/4.0/).

Abstract: In the present work, hybrid Cellulose Nanocrystal–MXene (CNC–MXene) nanolubricants were prepared via a two-step method and investigated as potential heat-transfer hybrid nanofluids for the first time. CNC–MXene nanolubricants were synthesized via a two-step method by varying the weight percentage of CNC–MXene nanoparticles (ranging from 0.01 to 0.05 wt%) and characterized using Fourier-Transform Infrared Spectroscopy and TGA (Thermogravimetric Analysis). Response surface methodology (RSM) was used in conjunction with the miscellaneous design model to identify prediction models for the thermophysical properties of the hybrid CNC–MXene nanolubricant. Minitab 18 statistical analysis software and Response Surface Methodology (RSM) based on Central Composite Design (CCD) were utilized to generate an empirical mathematical model investigating the effect of concentration and temperature. The analysis of variance (ANOVA) results indicated significant contributions from the type of nanolubricant ($p < 0.001$) and the quadratic effect of temperature ($p < 0.001$), highlighting non-linear interactions that affect viscosity and thermal conductivity. The findings showed that the predicted values closely matched the experimental results, with a percentage of absolute error below 9%, confirming the reliability of the optimization models. Additionally, the models could predict more than 85% of the nanolubricant output variations, indicating high model accuracy. The optimization analysis identified optimal conditions for maximizing both dynamic viscosity and thermal conductivity. The predicted optimal values (17.0685 for dynamic viscosity and 0.3317 for thermal conductivity) were achieved at 30 °C and a 0.01% concentration, with a composite desirability of 1. The findings of the percentage of absolute error (POAE) reveal that the model can precisely predict the optimum experimental parameters. This study contributes to the growing field of advanced nanolubricants by providing insights into the synergistic effects of CNC and MXene in enhancing thermophysical properties. The developed models and optimization techniques offer valuable tools for tailoring nanolubricant formulations to specific tribological applications, potentially leading to improved efficiency and durability in various industrial settings.

Keywords: thermophysical properties; cellulose nanocrystal (CNC); MXene; nanolubricant

1. Introduction

The ever-increasing demands on machinery efficiency and durability in various industrial applications have driven the continuous pursuit of advanced lubrication technologies. Among the promising avenues explored, nanolubricants have emerged as a focal point due to their unique properties and potential to revolutionize tribological systems [1]. In this context, the synergistic combination of Cellulose Nanocrystals (CNCs) and MXene in a hybrid nanolubricant presents a compelling avenue for enhancing tribological performance [2]. As the backbone of numerous industrial processes, tribological systems face challenges associated with friction, wear, and heat generation. Conventional lubricants, while effective, often fall short in meeting the evolving demands of modern machinery [3]. The integration of nanomaterials into lubricant formulations has garnered attention as a means to address these challenges [4]. In this study, we focus on the hybridization of CNC and MXene, two distinct nanomaterials renowned for their exceptional mechanical and thermal properties, respectively. CNC, derived from renewable sources, offers excellent mechanical strength and biodegradability [5]. On the other hand, MXene, a relatively new class of two-dimensional materials, has shown remarkable thermal and electrical properties [6]. The combination of these materials in a nanolubricant formulation potentially offers a unique balance of enhanced tribological performance and improved thermal management.

Evolution of productions in the area of development and optimization of systems relying on heat transfer causes the growing need to design and introduce optimum lubricant fluids with high efficiency. Hence, researchers have undertaken abundant endeavors in their empirical, numerical, and analytical studies in order to introduce optimized working fluids used in heat transfer systems [7–10]. One of the factors of energy damping in various industries is friction between moving elements; lubricants are used in order to decrease this friction. Today, because of the impact of lubricants in industries, studies on their properties in order to increase efficiency and decrease costs are highly inevitable. Previous studies on the characterization of nanolubricants using Thermogravimetric Analysis (TGA) and Fourier-Transform Infrared Spectroscopy (FTIR) have highlighted the importance of these techniques in understanding the thermal and chemical properties of nanolubricants. TGA has been widely used to investigate the thermal stability and decomposition profiles of nanolubricants by analyzing weight loss under controlled heating conditions. This method allows researchers to determine the temperature at which the lubricant begins to degrade, as well as the amount of residual material after heating. For example, Ahmed et al. [11] employed TGA to study the thermal behavior of copper oxide (CuO) nanoparticles dispersed in a base oil, finding that the addition of nanoparticles improved the thermal stability of the lubricant by delaying the onset of decomposition. Similarly, TGA has been used to evaluate the oxidative stability of nanolubricants, revealing that nanoparticles can enhance the lubricant's resistance to oxidation at elevated temperatures [12].

FTIR spectroscopy, on the other hand, has been utilized to study the chemical interactions between nanoparticles and base oils by identifying characteristic functional groups. FTIR helps in detecting the presence of specific chemical bonds and monitoring any changes that occur during the formulation or application of nanolubricants. Studies such as those by Patel et al. [13] have used FTIR to confirm the successful incorporation of nanoparticles into lubricants and to evaluate the chemical stability of the resulting nanolubricant. Additionally, FTIR has been instrumental in identifying potential chemical reactions between nanoparticles and lubricant additives, which can influence the performance of the nanolubricant. These studies have demonstrated that combining TGA and FTIR provides a comprehensive understanding of the thermal and chemical

properties of nanolubricants, facilitating the development of more efficient and durable lubrication solutions for industrial applications.

Response Surface Methodology (RSM) is the most preferred statistical tool to optimize the significant parameters of any real-time manufacturing process, as it requires a minimum set of experiments and provide optimum condition settings for maximum yield [14]. As RSM formulates a mathematical matrix and considers multiple variables and their interactions, it requires a lower number of experimental trails, as compared to ANN [15]. Therefore, using RSM, various studies successfully validated the experimental results without any assumptions. In one such study, Nasirzadehroshenin, Maddah [16] synthesized Al_2O_3-TiO_2 (10%) nanocomposite in three sizes and dispersed them in water to synthesize hybrid nanofluid with 0–0.5% volume fraction at 20–50 °C and successfully predicted thermal conductivity and viscosity using RSM and ANN. Analysis of variance (ANOVA) table confirmed that temperature (A), concentration (B), particle size (C) and interaction term (AB) showed a significant impact on the model with a lower *p*-value. Peng, Khaled [17] predicted and optimized the thermal conductivity of CuO/water nanofluid using RSM at ϕ = 0.1–0.4 vol% and 25–40 °C. Authors claimed that, for CuO/water nanofluid, the proposed model can extrapolate and interpolate the data with less than 2% accuracy.

This research aims to investigate the thermophysical properties of hybrid CNC–MXene nanolubricants, focusing on their dynamic viscosity and thermal conductivity. By employing a Design of Experiment (DOE) approach using Response Surface Methodology (RSM), the predictive models are developed for dynamic viscosity and thermal conductivity as a function of temperature and concentration [9]. Furthermore, the nanolubricant concentration to achieve the best balance of dynamic viscosity and thermal conductivity for tribology applications is determined [10]. The findings of this study will contribute to the growing body of knowledge on advanced nanolubricants and provide valuable information for the practical implementation in various industrial settings, especially in tribological application.

2. Experimental Methodology

2.1. Preparation and Characterization of CNC, MXene, and CNC–MXene Nanolubricant

This section will cover the study's materials, a method for characterizing nanoparticles, making a hybrid nanolubricant, and judging a nanolubricant's characterization. In addition, this part will describe the method employed in this research to determine FTIR and TGA analysis. The two-step procedure was chosen for this study's nanolubricant preparation. Nine distinct nanolubricant samples are made using the two-step method, with concentrations ranging from 0.01% to 0.05% of volume. The concentrations of 0.01%, 0.03%, and 0.05% CNC–MXene were selected based on a combination of factors, with the Design of Experiment (DOE) approach playing a central role. The DOE, specifically Response Surface Methodology (RSM), guided the selection of these concentrations to explore the effects of varying nanoparticle loadings on the nanolubricant's thermophysical properties. By choosing low, medium, and high levels within this range, the study aimed to systematically capture the influence of concentration on dynamic viscosity and thermal conductivity, allowing for the development of accurate empirical models. The selected range also ensured that the CNC–MXene nanoparticles could maintain stability and uniform dispersion within the base fluid without issues such as agglomeration or sedimentation, which are common at higher concentrations. Additionally, these concentrations align with those commonly used in previous research on nanolubricants, facilitating comparisons with existing studies and providing a benchmark for performance evaluation [2].

The single CNC, single MXene, and hybrid CNC–MXene nanoparticles utilized to prepare the nanolubricant are employed. This method uses base fluids of SAE 10W-40 to disperse nanoparticles, creating a stable, homogeneous solution. The initial step in

preparing nanolubricants, Step 1, was figuring out the volume needed for dilution to determine the correct volume of the base fluid to achieve the desired nanoparticle concentration; it is is a critical preparatory action before dispersion. The importance of this step lies in ensuring precise dilution, which directly influences the consistency and stability of the nanolubricant, using Equation (1):

$$\emptyset = \frac{\left[\frac{W_p}{\rho_p}\right]}{\left[\frac{W_p}{\rho_p} + \frac{W_{bf}}{\rho_{bf}}\right]} \quad (1)$$

where W_p stands for the weight of the nanoparticles in grammes, ρ_p for their density in g/cm^3, ρ_{bf} for their density in g/cm^3, and W_{bf} for their weight in grammes. Then, the dry blending of CNC and MXene powder produces CNC–MXene nanoparticles. After that, in Step 2, a stirrer was used to mix the nanoparticles in the base fluid. As recommended by other researchers [18–21], the nanolubricant was blended for up to 30 min. Additionally, sonication was applied to the sample of nanolubricants. In 200 mL of base oil SAE 40, volume fractions of 0.01, 0.03, and 0.05% were used to create CNC, Mxene, and CNC–MXene nanolubricants. The initial dispersion of CNC, MXene, and CNC–MXene nanoparticles into engine oil was carried out using a hotplate magnetic stirrer at a medium stirring rate continuously for 1 h at room temperature. Each nanolubricant solution was placed in an ultrasonic bath for around two hours. This contributes significantly to the nanolubricants' increased stability.

To measure the viscosity of the CNC–MXene hybrid nanolubricant, a rheometer is used for the measurements. The viscometer is calibrated, and the sample is placed in the instrument. Temperature control is essential for this process, so the sample is placed in a temperature-controlled water or oil bath to maintain a constant temperature, ranging from 30 °C to 100 °C. The viscosity measurements are taken at multiple temperatures to observe how the lubricant's viscosity changes with temperature. Each measurement is repeated three times to ensure accuracy, and the data are recorded. For measuring the thermal conductivity of the CNC–MXene nanolubricant, the thermal conductivity meter, using the transient hot-wire method, is employed. The nanolubricant sample is placed in the thermal conductivity testing chamber, and the instrument is calibrated to the desired temperature range. Just like in the viscosity measurement, a temperature-controlled bath is used to ensure the sample is tested in a range from 30 °C to 100 °C. The thermal conductivity of the sample is measured by observing how quickly heat is transferred through the nanolubricant. Multiple tests are performed at 0.01% to 0.05% and temperatures to assess the nanolubricant's performance across different conditions. The data are then analyzed to determine the relationship between the temperature and concentration for both responses, which were viscosity and thermal conductivity.

For the characterization of CNC–MXene hybrid nanolubricants, both FTIR (Fourier-Transform Infrared Spectroscopy) and TGA (Thermogravimetric Analysis) are crucial methodologies. For the FTIR analysis, samples were prepared by dispersing the CNC, MXene, and CNC–MXene hybrid nanolubricants in a potassium bromide (KBr) pellet medium to form a thin film suitable for measurement. The FTIR spectra were collected using Thermo Fisher Scientific Nicolet iS50in model in the range from 4000 cm^{-1} to 400 cm^{-1}, with a resolution of 4 cm^{-1}. Each spectrum was averaged over 64 scans to improve the signal-to-noise ratio, and baseline correction was applied. The spectra were analyzed to identify characteristic functional groups, such as C-H, O-H, and N-H, which indicate molecular interactions between the CNC, MXene, CNC–MXene and the base oil used in the nanolubricants.

For TGA analysis, TGA was used to analyze the thermal stability and composition of the nanolubricant by measuring the weight loss of the sample as it is heated at a controlled rate. Thermogravimetric analyzer model STA7000 Hitachi manufactured by Hitachi High-Tech Corporation, which is based in Tokyo, Japan was used under a nitrogen atmosphere

to prevent oxidation during heating. Approximately 10 mg of each nanolubricant sample was heated from room temperature to 800 °C, at a rate of 10 °C per minute. The weight loss of the samples was monitored as a function of temperature to determine the onset of thermal degradation and the residual mass after complete decomposition. This analysis was crucial in evaluating the thermal stability of the CNC, MXene, and hybrid CNC–MXene nanolubricants to compare the stability at different concentrations (0.01%, 0.03%, and 0.05%) and types of nanolubricant. Before the TGA analysis, the instrument was carefully calibrated to ensure accurate results. Nickel was used for temperature calibration, which was approximately 1455 °C. The TGA was run under the same conditions as the actual tests, and the melting point was checked against the temperature value. Any differences were adjusted in the instrument settings. For weight calibration, a platinum weight was used. The 20 mg weight was placed on the TGA balance, and the measured value was checked against the weight. To ensure the consistent accuracy, adjustments were made if there were any inconsistencies. To correct the baseline, an empty sample pan was run through the TGA cycle to adjust for any drift and ensure accurate heat flow measurements. The nitrogen gas flow rates and atmosphere settings were also checked to match the testing conditions. Finally, calibration was verified using a base fluid to confirm that the TGA was functioning correctly. These steps ensured that the TGA data were accurate and reliable, supporting the study's findings on the thermal stability of the nanolubricants.

2.2. Design of Experiment and Regression Modelling

The DOE was designed to develop empirical models that predict the thermophysical properties, which are the dynamic viscosity and thermal conductivity of the CNC–MXene nanolubricants, and to optimize these properties for tribological applications. This approach aimed to identify the best conditions that would enhance the efficiency and durability of the nanolubricant, making it suitable for various industrial applications. The study employed Response Surface Methodology (RSM), a statistical and mathematical technique that allows researchers to examine the relationships between multiple input variables and one or more response variables. RSM was chosen because it efficiently models and optimizes processes with minimal experimental runs, making it ideal for complex formulations like nanolubricants. The experimental factors chosen for this study included two continuous variables: temperature and concentration of the nanolubricant. Temperature was tested at three levels, low (30 °C), center (60 °C), and high (90 °C), to capture a range of operating conditions that could affect the nanolubricant's performance. The concentration of the nanolubricant was also evaluated at three levels, low (0.01%), center (0.03%), and high (0.05%), to understand how varying amounts of CNC–MXene nanoparticles influenced the lubricant's properties.

In addition to the continuous factors, the type of nanolubricant was considered as a categorical variable with three different types: pure CNC, pure MXene, and a hybrid CNC–MXene combination. This categorical factor allowed the researchers to assess the individual and combined effects of these nanoparticles on the lubricant's performance. The experimental design was based on the Central Composite Design (CCD), a type of RSM design that is particularly effective for fitting quadratic models and identifying interaction effects between factors. CCD is advantageous because it includes a mix of factorial points, axial points, and center points, which provide a comprehensive dataset for evaluating the main effects, quadratic effects, and interactions [22]. In total, 39 experimental runs were conducted, each designed to capture the response of the nanolubricant's dynamic viscosity and thermal conductivity under varying conditions.

Analysis of Variance (ANOVA)

The collected data were analyzed using analysis of variance (ANOVA) to determine the statistical significance of each factor and the factors' interactions. ANOVA helped validate the developed empirical models by showing which factors significantly

influenced the properties of the nanolubricant. The RSM models were further validated by comparing predicted values with experimental data, achieving high accuracy, with R-squared values above 85%, indicating a strong fit between the models and the actual results. Response surfaces can be evaluated to determine the minimum or maximum responses and the equivalent optimum conditions. The optimum circumstances can be found using various responses when all the parameters meet the desirable requirements simultaneously. Using multiple responses, the optimum conditions can be found when all the parameters simultaneously satisfy the desirable criteria. Furthermore, the optimum condition can be found graphically by superimposing the contour plots of the regression model in an overlay plot. The graphical optimization indicates the area of feasible response values in the factor space and the regions that fit the optimization criteria [23]. The confirmation experiment is essential to validate the model's accuracy between the measured experimental data and the regression analysis's predicted value. Kumar, Saravanan [24] reported that confirmation experiments are not necessary if the RSM models produce a prediction error of less than 5%. Furthermore, the percentage of absolute error (POAE) is used to measure the difference between the measured experimental results and the predicted value obtained from the regression model using Equation (2).

$$\text{POAE} \quad (\%) \quad = \left(\frac{\text{Actual} \quad \text{value - Predicted} \quad \text{value}}{\text{Actual} \quad \text{value}} \right) \times 100 \tag{2}$$

3. Result and Discussion

3.1. FTIR Evaluation and Thermogravimetric Analysis and of CNC, MXene, and CNC–MXene Nanolubricant

Figure 1 shows the transmittance (%) as a function of wave number (cm^{-1}) for the CNC–MXene hybrid at different concentrations, 0.01%, 0.03%, and 0.05%. The graph displays a distinct absorption peak around 2900–3000 cm^{-1}, which is typical for C-H stretching vibrations found in organic compounds. The intensity of the absorption peak varies slightly with the concentration, with the 0.05% CNC–MXene sample (blue line) showing the deepest absorption, indicating a higher concentration of C-H bonds or interactions in this sample.

The other samples, 0.01% (black line) and 0.03% (red line), show less pronounced peaks, suggesting a lower concentration of the corresponding functional groups. Above 3000 cm^{-1}, the transmittance levels off, indicating that there are no significant absorption features in this region for the samples tested. Below 2900 cm^{-1}, the transmittance drops sharply due to the absorption of infrared light by the material, which is characteristic of the chemical bonds present [25]. In summary, this FTIR spectrum indicates the presence of C-H bonds in the CNC–MXene nanolubricant, with varying concentrations affecting the presence and intensity of functional groups, particularly C-H bonds. This information is crucial for understanding the molecular interactions within the nanolubricant and optimizing its formulation for specific applications [26].

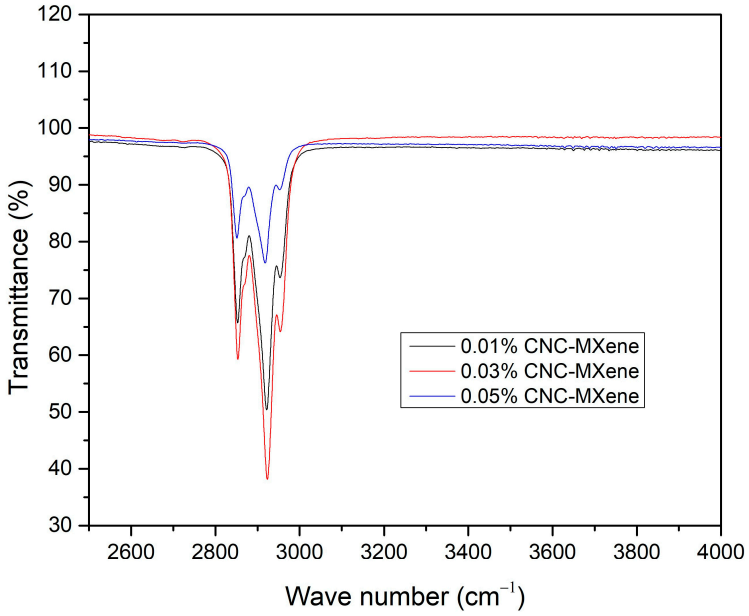

Figure 1. FTIR spectrum for CNC–MXene at different concentration (0.01%, 0.03%, and 0.05%).

Figure 2 shows the FTIR evaluation for the single nanolubricants (CNC and MXene) and hybrid nanolubricant (CNC–MXene) on the wave number region between 2600 cm^{-1} and 4000 cm^{-1}, where stretching vibrations of functional groups such as C-H, O-H, and N-H typically appear. The most prominent peaks are observed between 2800 cm^{-1} and 3000 cm^{-1}, which are attributed to C-H stretching vibrations, commonly associated with aliphatic hydrocarbons [27]. These C-H bonds are likely part of the base oil used in the nanolubricant, and the peaks are consistently present across all concentrations and materials, including CNC, MXene, and the CNC–MXene hybrid. As the concentration of CNC, MXene, or CNC–MXene increases, there is a noticeable rise in the intensity of these C-H stretching peaks. For instance, at lower concentrations, i.e., 0.01%, the intensity is relatively subdued, while at higher concentrations (0.03% and 0.05%), the peaks become more affirmed. This increase suggests that a greater number of nanoparticles in the lubricant system enhances the absorption of infrared radiation in this region.

Additionally, there are minor shifts in the exact wave number of the C-H stretching vibrations, particularly in the CNC–MXene hybrid nanolubricant. At the highest concentration (0.05%), the CNC–MXene hybrid nanolubricant shows slight shifts compared to the spectra of CNC or MXene alone, indicating some level of interaction between CNC and MXene. These shifts imply that the environment surrounding the C-H groups is altered slightly by the combination of these two nanoparticles. In the region above 3000 cm^{-1}, where O-H stretching vibrations typically appear between 3200 cm^{-1} and 3600 cm^{-1}, there are no significant broad peaks are observed. This suggests that hydroxyl groups, such as those present in the cellulose structure of CNC, do not have a dominant impact on the absorption in this region. The absence of these O-H peaks may indicate that CNC's functional groups do not significantly alter the lubricant's behavior at these concentrations.

In summary, the C-H stretching peaks are the dominant feature in this region, with increasing intensity reflecting higher nanoparticle concentrations. The minor shifts in peak positions for the CNC–MXene hybrid suggest potential interactions between CNC and MXene, although hydroxyl groups do not significantly contribute to absorption in the higher wave number region.

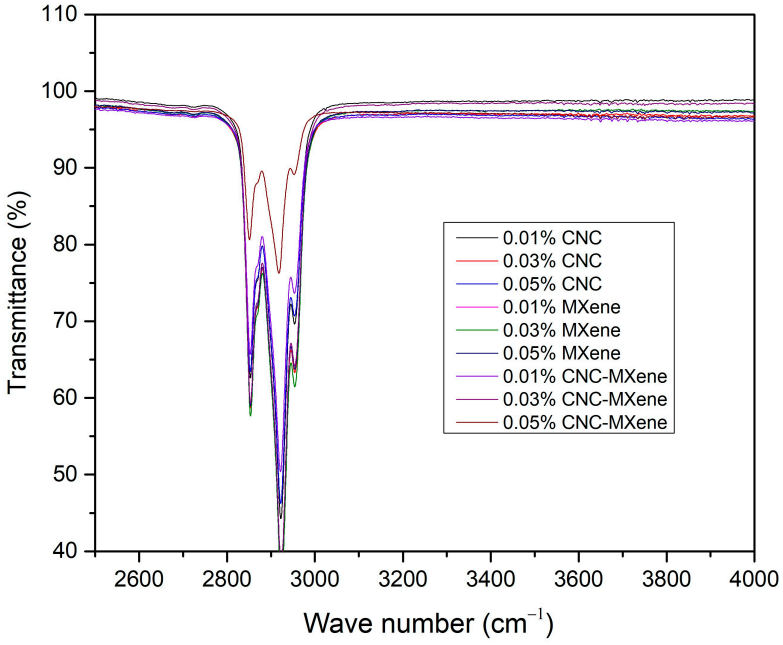

Figure 2. FTIR graph analysis for all concentrations of different types of nanolubricant.

Figure 3 presented here illustrates the thermal stability of CNC–MXene nanolubricants at different concentrations, which are 0.01%, 0.03%, and 0.05%. The graph plots the weight percentage remaining as a function of temperature, ranging from room temperature up to 600 °C. In the early stages, up to approximately 250 °C, there is minimal weight loss for all concentrations, indicating good thermal stability within this range, likely due to the evaporation of moisture or other volatile components. As the temperature increases beyond 250 °C, significant weight loss occurs, marking the onset of thermal degradation of the nanolubricant. The sharp decline in weight percentage between 250 °C and 400 °C represents the primary decomposition phase for the CNC–MXene nanolubricants. Among the concentrations, the 0.03% MXene–CNC sample (red line) experiences the most rapid degradation, with the lowest residual weight after the thermal event, suggesting that this concentration may have the least thermal stability.

In contrast, the 0.01% shows the highest residual weight, indicating better thermal stability among the three samples. The 0.05% falls between the other two, with moderate thermal stability. Beyond 400 °C, the curves start to plateau, showing the formation of more thermally stable residues. The 0.01% concentration leaves the most residue, while the 0.03% concentration leaves the least, supporting the observation that lower concentrations of CNC–MXene exhibit better thermal stability. Overall, this TGA analysis indicates that the thermal stability of CNC–MXene nanolubricants varies with the concentration. The 0.01% concentration provides the highest thermal stability, while the 0.03% concentration degrades the most rapidly. These results suggest that careful optimization of the MXene–CNC concentration is essential for enhancing the thermal performance of nanolubricants.

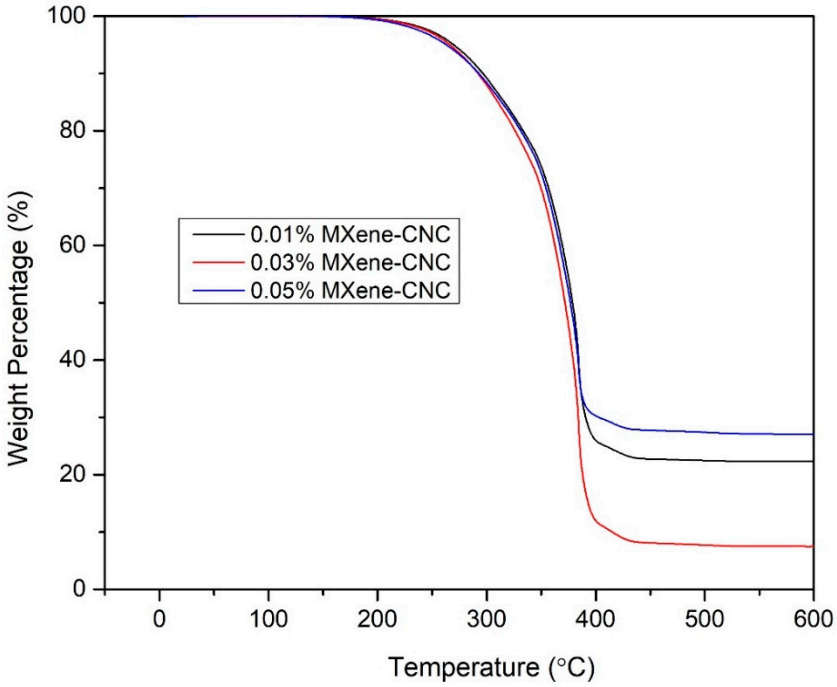

Figure 3. TGA graph of CNC–MXene at different concentrations.

Figure 4 illustrates the thermal stability of different samples, including CNC, MXene, and CNC–MXene nanolubricants, each at varying concentrations (0.01%, 0.03%, and 0.05%). The X-axis represents the temperature range from 0 °C to 600 °C, while the Y-axis shows the percentage of the initial sample weight remaining as the temperature increases. In the initial phase, up to around 200–250 °C, all samples exhibit minimal weight loss, indicating stability in this temperature range, typically associated with the removal of moisture and other unstable components. The most significant weight loss occurs between 250 °C and 400 °C, marking the decomposition of the materials. The CNC nanolubricant decomposes more rapidly than the MXene nanolubricant, suggesting that MXene has superior thermal stability. The CNC–MXene nanolubricant displays intermediate behavior, with better thermal stability than pure CNC, but slightly less than pure MXene. This indicates that incorporating MXene into CNC enhances the nanolubricant thermal properties.

At temperatures above 400 °C, the curves begin to level off, reflecting the amount of material that remains thermally stable and does not decompose further. MXene samples leave more residue than CNC, indicating a higher proportion of thermally stable material. The CNC–MXene nanolubricant leaves a moderate amount of residue, further highlighting the improved thermal stability compared to CNC alone, but still less than pure MXene. In summary, the TGA data show that MXene exhibits higher thermal stability compared to CNC, and the CNC–MXene nanolubricant offers enhanced thermal properties over pure CNC, making them potentially more suitable for applications requiring higher thermal resistance especially for tribological applications under cryogenics (−269 °C) to high-temperature (up to 1000 °C) environments [28].

The analysis revealed that incorporating MXene into the CNC nanoparticles enhanced the thermal stability of the hybrid nanolubricant compared to CNC, as MXene is known for its high thermal resistance. However, the stability varied with the concentration of CNC–MXene, highlighting the importance of optimizing nanoparticle loadings to achieve the best thermal performance. Overall, the TGA results shows that the CNC–MXene nanolubricant's thermal stability is concentration-dependent, and lower concentrations (0.01%) provided better thermal resistance, making them more suitable for applications where thermal stability is critical. This comprehensive analysis of thermal

stability contributes to our understanding of how CNC and MXene synergistically improve the durability and performance of nanolubricants under high-temperature conditions.

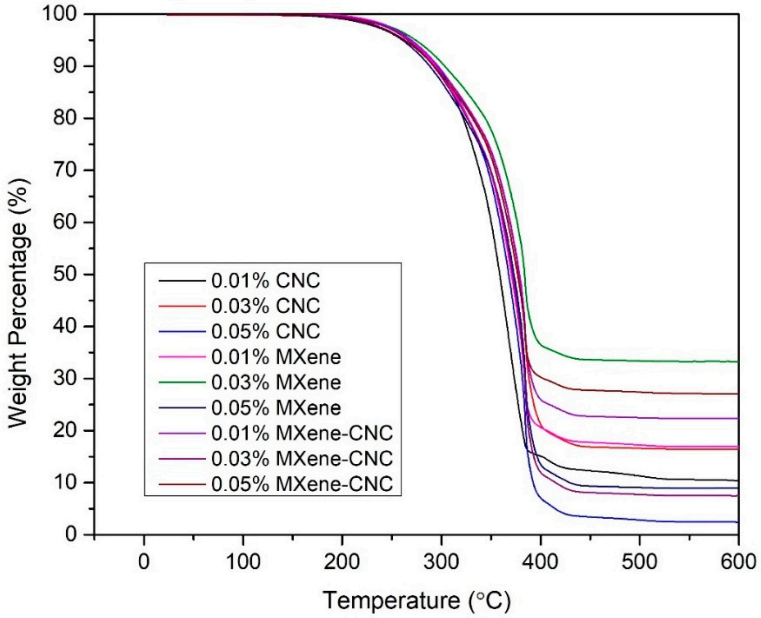

Figure 4. TGA graph analysis for varying concentrations (0.01%, 0.03%, and 0.005%) of CNC, MXene, MXene–CNC nanolubricants.

3.2. Statistical Approach for Prediction and the Optimization of Dynamic Viscosity and Thermal Conductivity Using Response Surface Methodology

In this section, the Response Surface Methodology method (RSM) is used to determine the prediction models for thermophysical properties of CNC, MXene, and CNC–MXene nanolubricant, i.e., dynamic viscosity, thermal conductivity, and specific heat capacity, and compared with the curve-fitting method. The RSM is a technique based on statistical and mathematical approaches for developing and optimizing the experimental data. This modelling approach is useful when several input parameters interact with each other, and the interaction affects the system's output, referred to as response. The input parameters are also referred to as independent variables. An RSM model will decrease the number of experiments required to understand the trend and behavior [29]. An experimental design was carried out using Minitab 18, developed by Minitab LLC, located in State College, PA, USA. This version was released in 2017. a statistical analyzing software, by referring to factors with various levels, as shown in Table 1. This experiment is designed by considering two continuous factors. Hence, the Central Composite Design (CCD) method is approached, suitable for developing models with two continuous factors. They are classified into three levels, low value (−1), high value (+1), and center value (0). The continuous factors are temperature (T) and volume concentration (Ø). Thirty-nine experiments were designed to study the influence of temperature, volume concentration, dynamic viscosity, thermal conductivity, and specific heat capacity. The design layout and experimental results are summarized in Table 2. StdOrder (Standard Order) is used to reflect the planned sequence of the experimental trials, as designed by the Central Composite Design (CCD) under Response Surface Methodology (RSM). RunOrder captures the actual order in which the experiments were conducted. This is crucial for tracking the execution of the trials, as it can reveal potential influences of time-dependent factors, such as environmental variations or equipment performance changes, on the results. Block-group experiments were conducted under similar conditions to manage variability that could arise from changes over time or other external factors. In

this study, blocking helps control the effect of these variations, allowing for a more accurate analysis of the primary factors—temperature, concentration, and type of nanolubricant—by reducing the impact of irrelevant noise. PtType (Point Type) indicates the specific type of experimental points used in the design, including factorial, center, and axial points. These point types are essential in the CCD, as they define the structure of the experimental space. Together, these columns ensure that the experimental design is properly executed and statistically sound, providing a comprehensive framework for optimizing the thermophysical properties of the CNC–MXene nanolubricants.

Table 1. Factors at various levels.

Continuous Factors	−1	0	+1
Temperature (continuous)	30	60	90
Concentration (continuous)	0.1	0.5	0.9
Categorical factors	−1	0	+1
Type of nanolubricant	CNC	MXene	CNC–MXene

Table 2. Design of experiment, along with experimental results.

StdOrder	RunOrder	Blocks	PtType	Temperature	Concentration	Type of Nanolubricant	Viscosity	Thermal Conductivity
1	1	1	1	30	0.01	MXene	41.08145	0.3801
2	2	1	1	70	0.03	MXene	79.56635	1.7506
3	3	1	1	70	0.03	MXene	79.56635	1.7506
4	4	1	1	70	0.03	CNC–MXene	114.4096	1.46509
5	5	1	1	70	0.05	MXene	98.86867	0.33891
6	6	1	1	70	0.03	CNC	41.14307	1.7506
7	7	1	1	70	0.03	MXene	79.56635	1.7506
8	8	1	1	30	0.03	CNC–MXene	114.4096	0.43682
9	9	1	1	70	0.03	CNC–MXene	114.4096	1.46509
10	10	1	1	100	0.05	CNC	47.16928	3.64706
11	11	1	1	70	0.01	CNC–MXene	98.77636	2.37387
12	12	1	1	100	0.01	CNC	48.91227	1.6185
13	13	1	1	70	0.03	CNC–MXene	114.4096	1.46509
14	14	1	1	70	0.03	MXene	79.56635	1.7506
15	15	1	1	30	0.01	CNC–MXene	40.85564	0.37413
16	16	1	1	100	0.01	CNC–MXene	46.51977	2.26471
17	17	1	1	30	0.03	MXene	79.56635	0.35821
18	18	1	1	70	0.05	CNC	80.13515	1.45494
19	19	1	1	70	0.03	CNC	41.14307	1.7506
20	20	1	1	70	0.03	CNC	41.14307	1.7506
21	21	1	1	30	0.01	CNC	41.67993	0.38507
22	22	1	1	100	0.05	CNC–MXene	42.67204	0.73743
23	23	1	1	100	0.05	MXene	48.5423	0.29837
24	24	1	1	70	0.01	CNC	42.57501	0.56324
25	25	1	1	30	0.05	MXene	42.4807	0.37015
26	26	1	1	100	0.01	MXene	48.84116	0.83717
27	27	1	1	30	0.05	CNC–MXene	44.97446	0.36816
28	28	1	1	70	0.03	MXene	79.56635	1.7506
29	29	1	1	70	0.03	CNC	41.14307	1.7506
30	30	1	1	70	0.03	CNC	41.14307	1.7506
31	31	1	1	30	0.05	CNC	41.81186	0.37612
32	32	1	1	100	0.03	MXene	40.51796	2.15814
33	33	1	1	100	0.03	CNC–MXene	47.88457	1.79028
34	34	1	1	70	0.05	CNC–MXene	122.3274	0.62611
35	35	1	1	70	0.03	MXene	79.5663	1.7506
36	36	1	1	70	0.03	CNC–MXene	114.4096	1.46509
37	37	1	1	100	0.03	CNC	27.96678	0.95396
38	38	1	1	30	0.03	CNC	21.14307	0.40597
39	39	1	1	70	0.03	CNC–MXene	114.4096	1.46509

3.2.1. ANOVA Analysis for Dynamic Viscosity and Thermal Conductivity

Table 3 shows the ANOVA table provided to analyze the effect of temperature, concentration, and type of nanolubricant on the dynamic viscosity of the CNC–MXene nanolubricant. The model accounts for 69.47% of the total variability in viscosity, as indicated by the Sequential Sum of Squares (Seq SS) of 23,995.8. The model's total F-value of 5.58 and a *p*-value of 0 suggest that the model is statistically significant overall; however, further examination of individual components reveals mixed results. Specifically, the ANOVA results showed that the type of nanolubricant had a strong influence on viscosity (F-value of 16.6 and *p*-value < 0.001), contributing significantly to the model's overall variation. However, other factors, such as temperature and concentration in their linear forms, had minimal impacts, with high *p*-values ($p > 0.3$), indicating that these factors were not statistically significant on their own. Additionally, the interaction effects and some quadratic terms were not significant, further highlighting the inconsistencies in the significance of the overall model components. The linear model explains 38.32% of the variation, and it is also highly significant, whereas the *p*-value is 0, driven mainly by the type of nanolubricant, which contributes 36.72% to the total variation in viscosity. The F-value of 16.6 for the type of nanolubricant indicates a strong influence on viscosity, with a *p*-value of 0, thus confirming its significance. On the other hand, temperature and concentration individually have minimal contributions, with 0.09% and 1.51% of the variation, respectively. Their *p*-values, which are 0.418 for temperature and 0.356 for concentration, indicate that neither of these factors is statistically significant in their linear form.

The square terms contribute 30.22% of the variation in viscosity, with the quadratic effect of temperature (T^2) being highly significant. The temperature quadratic term alone contributes 30.21% to the total variation, with a very high F-value of 21.17 and a *p*-value of 0, indicating a strong non-linear relationship between temperature and viscosity. In contrast, the quadratic effect of concentration (C^2) is negligible, contributing only 0.01% with a non-significant *p*-value of 0.925. As for the interaction effect, the two-way interaction effects contribute only 0.93% of the variation, with none of the interaction terms being significant. The interactions between temperature and concentration (TC), temperature and type of nanolubricant (T × type), and concentration and type of nanolubricant (C × type) all have *p*-values far above 0.05, indicating that these interactions do not have a meaningful impact on viscosity.

The error term explains 30.53% of the variation, with a mean square error (MSE) of 390.64. Notably, the lack of fit is significant, indicating that the model does not perfectly fit the data, as shown by the high lack-of-fit F-value of 6.781. However, there is no contribution from pure error, meaning that the variability in the model is captured entirely by the fitted model and lack of fit. In conclusion, the results show that the type of nanolubricant and the quadratic effect of temperature are the most significant factors influencing dynamic viscosity, with the concentration and temperature having minimal linear effects. No significant interactions were found between the variables. The significant lack of fit suggests that there may be some additional complexity in the data that the model does not fully capture.

Table 4 shows the model summary for dynamic viscosity. The model summary indicates that the regression model provides a good fit to the data, as reflected by the statistical metrics. The standard error of the regression (S) is 0.0000197646, suggesting that the average distance of the observed values from the regression line is minimal, which implies a strong fit of the model to the data points. The R-squared value is 89.47%, meaning that 89.47% of the variation in the dependent variable is explained by the independent variables in the model, demonstrating a high level of explanatory power. Additionally, the adjusted R-squared value of 87.03% accounts for the number of predictors in relation to the number of observations. This slightly lower value compared to the R-squared indicates that while the model remains robust, some adjustment is made to account for potential overfitting due to the number of predictors used. Finally, the

Prediction Sum of Squares (PRESS) value is 0.00000805, which further supports the model's predictive capability, showing that it has a low error when predicting new data points. Overall, the high R-squared and adjusted R-squared values, combined with a low standard error, suggest that the model effectively captures the relationship between the variables, offering a strong explanatory power and a good fit to the data.

Table 3. ANOVA results for dynamic viscosity.

Source	DF	Seq SS	Contribution	Adj SS	Adj MS	F-Value	*p*-Value
Model	11	23,995.8	69.47%	23,995.8	2181.43	5.58	0
Linear	4	13,236.3	38.32%	13,594.2	3398.55	8.7	0
Temperature (T)	1	30.9	0.09%	264.3	264.32	0.68	0.418
Concentration (C)	1	521.2	1.51%	344.6	344.62	0.88	0.356
Type of nanolubricant	2	12,684.1	36.72%	12,966.5	6483.23	16.6	0
Square	2	10,438.7	30.22%	10,436	5218.02	13.36	0
T^2	1	10,434	30.21%	8271.1	8271.14	21.17	0
C^2	1	4.7	0.01%	3.6	3.57	0.01	0.925
2-way interaction	5	320.8	0.93%	320.8	64.15	0.16	0.974
TC	1	1.1	0.00%	1.1	1.14	0	0.957
T × type of nanolubricant	2	301.5	0.87%	301.4	150.7	0.39	0.684
C × type of nanolubricant	2	18.2	0.05%	18.2	9.11	0.02	0.977
Error	27	10,547.2	30.53%	10,547.2	390.64		
Lack of fit	14	10,547.2	30.53%	10,547.2	753.37		6.781
Pure error	13	0	0.00%	0	0		
Total	38	34,543	100.00%				

Table 4. Model summary for dynamic viscosity.

S	R-sq	R-sq(adj)	PRESS	R-sq(pred)
0.0000197646	89.47%	87.03%	0.00000805	0.00%

Generally, the model can fit the data with the highest R-squared (R^2) and adjusted R-squared (R^2-adj) value. R^2, the coefficient of determination, is the ratio of the changes described by the model to the whole changes. Therefore, whenever the value of R^2 is closer to one, the power of the fitted model describing the response changes as a function of the independent variables is greater [30]. For a model with a good fitting, the R^2 should be at least 80% [31]. In the dynamic viscosity and thermal conductivity analysis study, the determining factors of the model for thermal conductivity are 89.97% and 87.97% for R^2 (adj), respectively. Hence, the model correlates the experimental data accurately.

Table 5 shows the ANOVA table that analyzes the effects of temperature, concentration, and the type of nanolubricant on a particular response variable. The model explains 66.02% of the total variability in the response, as indicated by the Sequential Sum of Squares (Seq SS) of 14.637. The model is statistically significant, with an F-value of 4.77 and a *p*-value of 0, indicating that the factors included in the model significantly affect the responses. The linear effects explain 35.66% of the total variation, with a significant *p*-value of 0.001. Among the linear terms, temperature has the most substantial contribution, accounting for 33.30% of the total variation, with a high F-value of 23.44 and a *p*-value of 0, indicating that temperature strongly influences the response variable. In contrast, concentration only contributes 0.96%, and its *p*-value of 0.39 shows that it is not statistically significant in the linear model. Similarly, the type of nanolubricant contributes a minor 1.41% and is also not significant, with a *p*-value of 0.653. The quadratic terms contribute 12.36% of the total variation and are significant overall, with a *p*-value of 0.015. The quadratic effect of temperature (T^2) explains 8.89% of the variation, but its *p*-value of

0.091 indicates that it is not statistically significant at the 5% level, though it shows some potential influence. The quadratic effect of concentration (C^2) contributes 3.47%, with a *p*-value of 0.13, indicating it is also not statistically significant.

The two-way interactions account for 17.99% of the total variation and are significant overall, with a *p*-value of 0.034. However, individual interaction terms show varying degrees of influence. The interaction between temperature and concentration (TC) contributes an insignificant 0.01% to the variation, with a *p*-value of 0.914. The interaction between temperature and type of nanolubricant explains 2.61%, but it is not significant, with a *p*-value of 0.372. In contrast, the interaction between concentration and type of nanolubricant is highly significant, accounting for 15.38% of the variation, with an F-value of 6.11 and a *p*-value of 0.006, indicating that the combination of concentration and type of nanolubricant has a meaningful effect on the response. The error term explains 33.98% of the variation, with a mean square error (MSE) of 0.27906. The lack of fit is significant, with an F-value of 4.7811, indicating that the model does not perfectly fit the data. This suggests that additional complexity or factors not included in the model may be influencing the response variable. The results show that temperature has the most significant impact on the response in the linear model, while concentration and type of nanolubricant have minimal direct effects. The quadratic effects, particularly for temperature, and the interaction between concentration and type of nanolubricant are important in explaining the variability in the response. However, the significant lack of fit indicates that the model may need further refinement to fully capture the behavior of the system.

Table 5. ANOVA results for thermal conductivity.

Source	DF	Seq SS	Contribution	Adj SS	Adj MS	F-Value	*p*-Value
Model	11	14.637	66.02%	14.637	1.33064	4.77	0
Linear	4	7.9073	35.66%	7.0208	1.75519	6.29	0.001
Temperature (T)	1	7.3823	33.30%	6.5412	6.54121	23.44	0
Concentration (C)	1	0.2118	0.96%	0.2127	0.21265	0.76	0.39
Type of nanolubricant	2	0.3133	1.41%	0.2416	0.12079	0.43	0.653
Square	2	2.7401	12.36%	2.734	1.36702	4.9	0.015
T^2	1	1.9712	8.89%	0.8571	0.85712	3.07	0.091
C^2	1	0.7689	3.47%	0.68	0.68004	2.44	0.13
2-way interaction	5	3.9896	17.99%	3.9896	0.79791	2.86	0.034
TC	1	0.0027	0.01%	0.0033	0.00328	0.01	0.914
T × type of nanolubricant	2	0.5776	2.61%	0.572	0.28599	1.02	0.372
C × type of nanolubricant	2	3.4093	15.38%	3.4093	1.70463	6.11	0.006
Error	27	7.5345	33.98%	7.5345	0.27906		
Lack of fit	14	7.5345	33.98%	7.5345	0.53818		4.7811
Pure error	13	0	0.00%	0	0		
Total	38	22.1716	100.00%				

Table 6 presented a comprehensive evaluation of the regression model's fit. The standard error (S) of 0.000528258 indicates that the residuals, or errors between the observed and predicted values, are very small. This low value suggests that the model's predictions closely match the actual data, reflecting a good fit. The R-squared (R-sq) value of 96.02% shows that the model explains a substantial 96.02% of the variation in the response variable. This high R-squared value signifies that the model fits the data very well, capturing most of the variability. The adjusted R-squared (R-sq adj), which accounts for the number of predictors, is 92.17%, slightly lower than the R-squared but still indicating a strong model fit. The drop between R-squared and adjusted R-squared

reflects the penalty for including additional predictors that may not contribute significantly to the model.

The Predicted Residual Sum of Squares (PRESS) value of 0.000267149 measures how well the model predicts new data points, with lower values indicating better predictive accuracy. In summary, the model explains the variation in the data well, as indicated by the high R-squared and adjusted R-squared values, and the low standard error suggests accurate predictions within the data used for the analysis. These results suggest that the model has a strong fit and adequately captures the underlying relationships in the data.

Table 6. Model summary for thermal conductivity.

S	R-sq	R-sq(adj)	PRESS	R-sq(pred)
0.000528258	96.02%	92.17%	0.000267149	69.00%

3.2.2. Development of Proposed Regression Model

Applying RSM would be useful to create a mathematical model that describes how the viscosity and thermal conductivity (response variable) change with the temperature and concentration (independent variables) [32]. The model would likely be a second-order polynomial equation: Equations (3)–(5) describe the relationship between the thermal conductivity of different nanolubricants (CNC, CNC–MXene, and MXene) and the variables temperature (T) and concentration (C). Each equation follows a similar polynomial form, incorporating both linear and quadratic terms for temperature and concentration, as well as an interaction term (TC) that captures the combined effect of temperature and concentration on thermal conductivity. Equation (3) denotes the models for thermal conductivity of a CNC nanolubricant. The positive coefficients for the linear terms of temperature (0.0603) and concentration (70.6) indicate that both increasing temperature and concentration tend to increase the thermal conductivity. However, the negative coefficients for the quadratic terms suggest diminishing returns or a decrease in thermal conductivity at higher temperatures and concentrations, potentially due to the non-linear behavior of the material. The interaction term represents the combined effect of temperature and concentration, where a negative value suggests that, at higher values of both variables, the thermal conductivity may decrease.

For the CNC–MXene nanolubricant in the Equation (4), the linear coefficients for temperature (0.0539) and concentration (19.0) are positive, indicating that an increase in these variables generally increases thermal conductivity. However, compared to the CNC nanolubricant, the effect of concentration is much smaller, suggesting that the CNC–MXene combination may not be as sensitive to changes in concentration. The quadratic and interaction terms are identical to those in Equation (2), implying similar diminishing returns and combined effects at higher levels of temperature and concentration.

Equation (5) for MXene nanolubricant also shows positive linear coefficients for temperature (0.0479) and concentration (32.4), indicating that both variables positively impact thermal conductivity. The magnitude of the concentration coefficient lies between those of CNC and CNC–MXene, suggesting a moderate sensitivity of thermal conductivity to changes in concentration. The quadratic and interaction terms are consistent with the other two equations, again reflecting the complex, non-linear relationship between these variables and the thermal conductivity of the MXene nanolubricant. In conclusion, all three equations share a common structure, with positive linear effects from temperature and concentration, and negative quadratic and interaction effects. This suggests that while increasing temperature and concentration generally enhances the thermal conductivity of the nanolubricants, there are diminishing returns at higher levels, potentially due to the intrinsic properties of the materials or the nature of heat transfer at elevated conditions. The differences in the coefficients, particularly for the concentration term, highlight the varying sensitivities of CNC, CNC–MXene, and MXene nanolubricants to these factors.

$$CNC = -2.516 + 0.0603\ T + 70.6\ C - 0.000278\ T^2 - 747\ C^2 - 0.024\ TC \quad (3)$$

$$CNC–MXene = -0.678 + 0.0539\ T + 19.0\ C - 0.000278\ T^2 - 747\ C^2 - 0.024\ TC \quad (4)$$

$$MXene = -0.753 + 0.0479\ T + 32.4\ C - 0.000278\ T^2 - 747\ C^2 - 0.024\ TC \quad (5)$$

These regression models describe the behavior of CNC, CNC–MXene, and MXene nanolubricants as a function of temperature (T), concentration (C), and the interaction of temperature and concentration (TC). Each equation follows a similar polynomial structure, including linear and quadratic terms for both temperature and concentration, as well as an interaction term between these two variables. Starting with the CNC model (Equation (6)), the intercept is −70.4, indicating the baseline value when both the temperature and concentration are zero. The temperature has a positive linear coefficient of 3.601, showing that as the temperature increases, the CNC values increase. However, this effect is moderated by the negative quadratic term (−0.02730 T^2), which suggests a diminishing return at higher temperatures. The concentration has a strong positive linear effect (432), but this is countered by a large negative quadratic term (−1711 C^2), indicating that the increase in CNC with concentration is only significant up to a certain point. The interaction term between temperature and concentration is negative (−0.44 TC), implying that the combined effect of temperature and concentration slightly reduces CNC compared to the effect of each variable individually.

The CNC–MXene model (Equation (7)) is similar but with a lower intercept of −4.1, indicating a different baseline when the temperature and concentration are zero. The coefficients for temperature (3.317) and concentration (331) are slightly lower than in the CNC model, suggesting a somewhat less pronounced response to changes in these variables. The quadratic and interaction terms remain identical across all three models, indicating that the non-linear effects of temperature and concentration, as well as their interaction, are consistent in all cases. The MXene model (Equation (8)) has an intercept of −31.7, and its coefficients for temperature (3.440) and concentration (315) fall between those of the CNC and CNC–MXene models. This indicates that the MXene nanolubricant's behavior is intermediate between the other two materials in terms of their response to temperature and concentration. Again, the quadratic and interaction terms are the same, suggesting a common pattern in the way these nanolubricants respond to varying temperature and concentration levels. Overall, these equations reveal that while the general form of the relationship between the variables is consistent across all three materials, the magnitude of their response to changes in temperature and concentration varies, reflecting the unique properties of CNC, CNC–MXene, and MXene nanolubricants.

Dynamic viscosity:

$$CNC = -70.4 + 3.601\ T + 432\ C - 0.02730\ T^2 - 1711\ C^2 - 0.44\ TC \quad (6)$$

$$CNC–Mxene = -4.1 + 3.317\ T + 331\ C - 0.02730\ T^2 - 1711\ C^2 - 0.44\ TC \quad (7)$$

$$MXene = -31.7 + 3.440\ T + 315\ C - 0.02730\ T^2 - 1711\ C^2 - 0.44\ TC \quad (8)$$

3.2.3. Surface Plot and Contour Plot

The surface plot, as shown in Figure 5, demonstrates the relationship between the thermal conductivity, temperature, and concentration of the nanolubricant. The x-axis represents the temperature, ranging from approximately 40 °C to over 100 °C, while the y-axis indicates the concentration, varying from 0.01% to 0.05%. The z-axis shows the thermal conductivity, which increases as both the temperature and concentration rise. As observed from the plot, the thermal conductivity improves with an increase in temperature. The upward slope of the surface indicates that higher temperatures lead to enhanced thermal energy transfer, likely due to increased molecular motion within the

nanolubricant. Similarly, higher concentrations of the nanolubricant contribute to better thermal conductivity, as the presence of more nanoparticles improves heat-transfer efficiency. The highest thermal conductivity value recorded was 0.3317 W/m·K. This indicates that higher temperatures combined with an increased nanoparticle concentration significantly boost heat-transfer capabilities, possibly due to the better dispersion and higher thermal conductivity properties of the MXene nanoparticles.

The combined effect of temperature and concentration reveals that both factors positively influence thermal conductivity, though temperature seems to have a more pronounced impact. The surface plot suggests that, at higher temperatures and concentrations, the nanolubricant exhibits significantly improved thermal conductivity, with temperature being the dominant factor in enhancing the heat-transfer properties

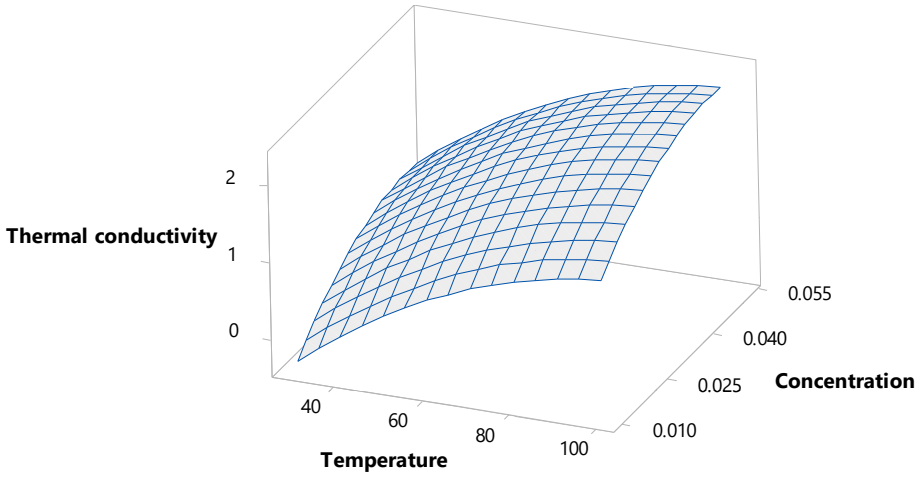

Figure 5. Surface plot for thermal conductivity.

The contour plot in Figure 6 illustrates the relationship between concentration, temperature, and thermal conductivity for a CNC-based nanolubricant. The x-axis represents the temperature, ranging from 30 °C to 100 °C, while the y-axis represents the concentration, ranging from approximately 0.012% to 0.048%. The plot is color-coded to represent different levels of thermal conductivity, with red indicating the lowest conductivity (<0.0 W/m·K) and purple indicating the highest (>2.0 W/m·K). The contour lines show how thermal conductivity changes with varying temperature and concentration. At lower temperatures (30 °C to 50 °C) and lower concentrations (around 0.012% to 0.024%), the thermal conductivity is lower, as indicated by the red and yellow regions. As both the temperature and concentration increase, the thermal conductivity improves, transitioning through yellow (0.5 to 1.0 W/m·K), light blue (1.0 to 1.5 W/m·K), and blue (1.5 to 2.0 W/m·K) regions.

Notably, the plot shows a strong dependence of thermal conductivity on both temperature and concentration. The highest thermal conductivity values (>2.0 W/m·K), represented by the purple region, are observed at higher temperatures (above 80 °C) and higher concentrations (around 0.042% and above). This suggests that increasing both the concentration of the CNC-based nanolubricant and the operating temperature enhances its thermal conductivity, making it more effective in heat-transfer applications under these conditions.

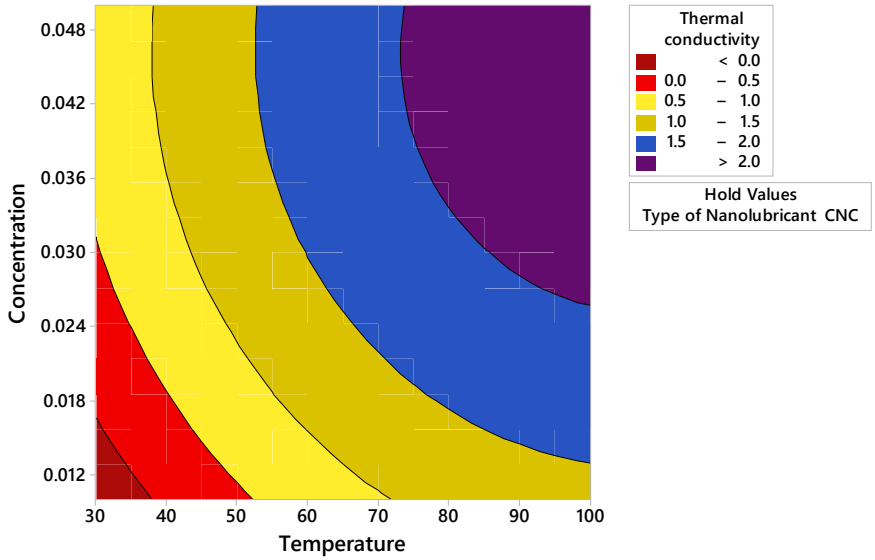

Figure 6. Contour plot for thermal conductivity.

Figure 7 illustrates the relationship between viscosity, temperature, and concentration in a three-dimensional space or surface plot. The plot shows that viscosity is influenced by both temperature and concentration in a non-linear manner. As the temperature increases from lower values, the viscosity initially rises, reaching a peak at around 80–100 °C, after which it declines as the temperature continues to rise. This creates a parabolic curve, indicating that there is an optimal temperature range for maximizing viscosity. In terms of concentration, higher concentrations (ranging from 0.01% to 0.05%) tend to increase viscosity, though the relationship appears more gradual and less steep compared to temperature's effect.

The plot also highlights an interaction between temperature and concentration, where the maximum viscosity is 17.0685 mPa·s. This indicates that higher temperatures combined with an increased nanoparticle concentration significantly boost heat-transfer capabilities, possibly due to better dispersion and higher thermal conductivity properties of the MXene nanoparticles. A good result is achieved when the temperature is moderate and the concentration is relatively high. Beyond this optimal region, further increases in temperature lead to a decline in viscosity, even at high concentrations. This interaction suggests that both variables must be balanced to optimize viscosity. Overall, the plot reflects the behavior predicted by the earlier regression equations, which include quadratic terms for both temperature and concentration, as well as an interaction term. The negative quadratic term for temperature explains the observed peak in viscosity, while the positive linear terms for both variables describe their initial influence on the increasing viscosity. This surface plot provides a clear visual representation of how viscosity depends on the interplay between temperature and concentration.

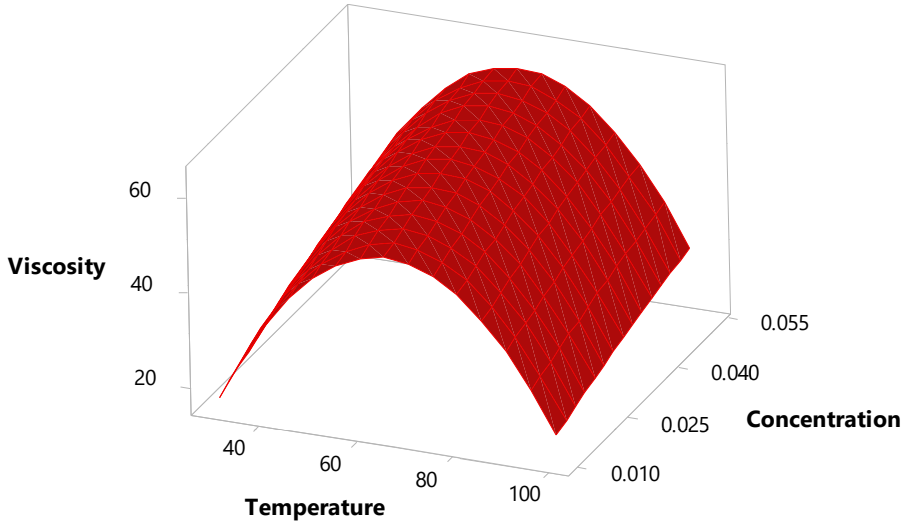

Figure 7. Surface plot for dynamic viscosity.

Figure 8 shows that the viscosity behavior of the CNC–MXene hybrid nanolubricant exhibits complex relationships with temperature and concentration. As the temperature increases from 30 °C to 100 °C, the viscosity generally decreases, following typical lubricant behavior. However, the concentration of the CNC–MXene nanolubricant significantly influences this trend. At higher concentrations of around 0.05%, the nanolubricant maintains high viscosity, which is (>60) in the mid-temperature range (60–80 °C), forming a distinctive U-shape in the viscosity distribution. At lower concentrations, 0.03%, the result in generally lower viscosities across all temperatures. The lubricant demonstrates the lowest viscosity (<20) at extreme conditions—either low concentrations with high temperatures or low concentrations with low temperatures. This diverse viscosity profile suggests that the CNC–MXene hybrid nanolubricant could be tailored for applications requiring specific viscosity characteristics under varying temperature and concentration conditions.

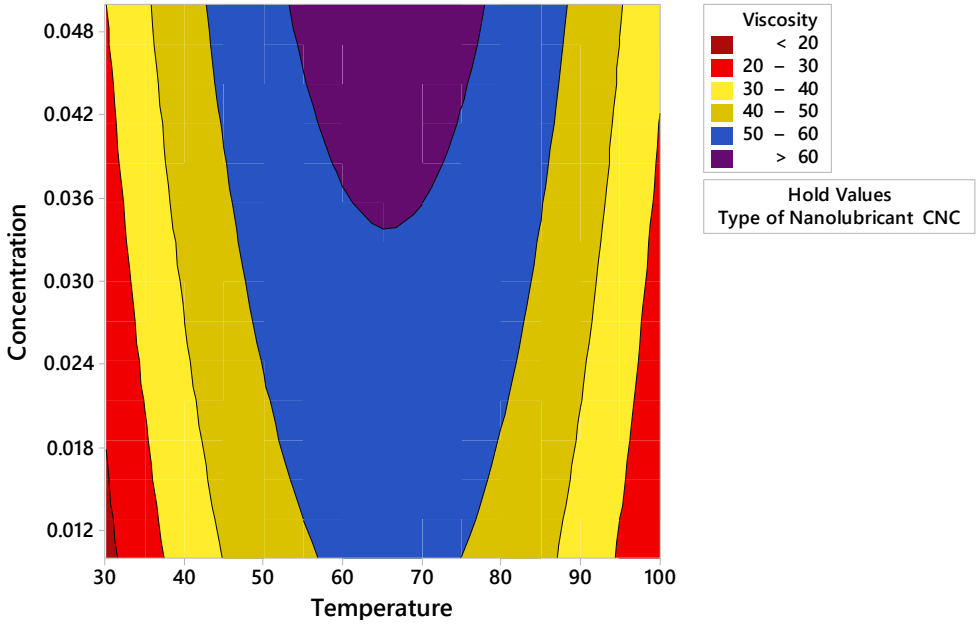

Figure 8. Contour plot for dynamic viscosity.

3.2.4. Comparison between Predicted and Experimental Model

Figure 9 and Figure 10 compares the experimental results of dynamic viscosity with the data predicted by the regression model. The graph depicts the relationship between experimental and correlation values using several key elements. The red line in the center, known as the line of equality, represents perfect correlation, meaning that if a point lies on this line, the experimental and correlation values are exactly equal. This line serves as a reference for how well the data fits the expected outcome. Surrounding the red line are dashed lines, which likely represent confidence intervals and the blue circles represent individual data points, each corresponding to an experimental value plotted against its respective correlation value. As can be seen, there is a good agreement between the model and experimental data. Therefore, there is a good correlation between the experimental and predicted results using the statistical method. Similarly, in Figure 10, the experimental data of thermal conductivity are compared to the data predicted by the regression model. As seen in both figures, the model predicts the experimental data well. The ineffective terms removed from the model are predicted well, and eliminating them has no adverse effect on the accuracy of the model.

The margin of deviation between the experimental and correlation results for all responses was also defined. The two response graphs show the calculated margin of deviation between experimental results and empirical equations at different volume concentration and temperatures. According to all of the figures, most points are located on the bisector or close to it, indicating the good accuracy of this equation. Moreover, the maximum margin of deviation, which is 1.3845 for dynamic viscosity and 0.897 for thermal conductivity, is shown in this diagram. This value is acceptable for an empirical equation. As can be seen, the forecasted values are a reasonable compromise with the experimentally obtained values. Also, as previously stated, most of the data points are on the 45-degree line, indicating a small difference between the experimental and predicted data [17]. As a result, the developed model is reliable.

In the comparison figures (Figures 9 and 10) from the study, the R-squared (R^2) values were used to evaluate how well the predicted models matched the experimental data for dynamic viscosity and thermal conductivity, respectively. For Figure 9, which compares the experimental and predicted values of dynamic viscosity, the R^2 value was reported to be high, reflecting that the model could explain a significant proportion of the variability in the experimental data. Specifically, the R^2 value for dynamic viscosity was approximately 89.47%, indicating that 89.47% of the variance in dynamic viscosity was accounted for by the model. This high R^2 value suggests that the model provides a good fit to the experimental data, with minimal deviations. For Figure 10, which compares the experimental and predicted values of thermal conductivity, the R^2 value was even higher, reported as approximately 96.02%. This indicates that the model explained 96.02% of the variability in the experimental thermal conductivity data. The high R^2 value demonstrates that the predictive model for thermal conductivity closely aligns with the experimental results, validating its accuracy and effectiveness. Overall, the R^2 values in both figures highlight the models' strong predictive capabilities, confirming that they reliably capture the relationship between the variables and can accurately forecast the thermophysical properties of the CNC–MXene nanolubricant.

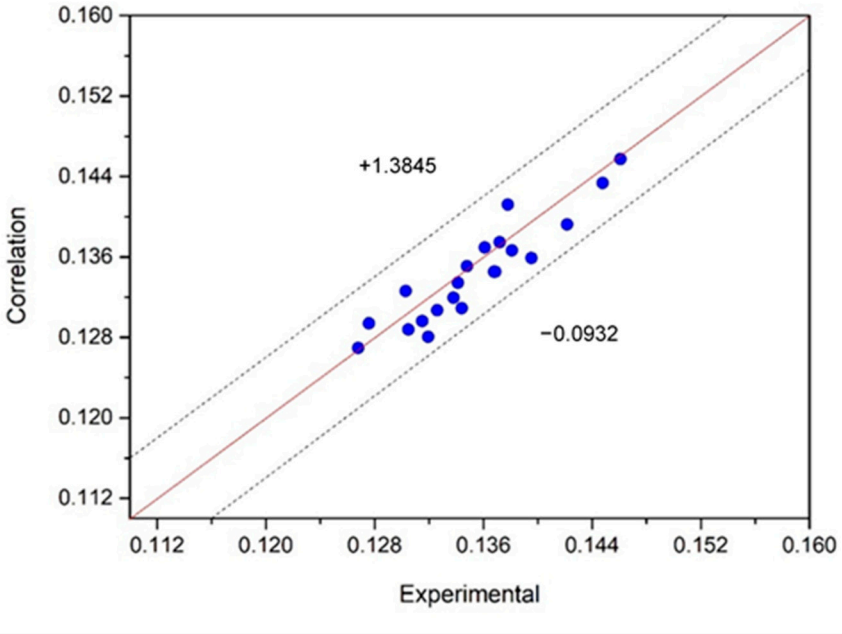

Figure 9. Comparison of the experimental and predicted model for dynamic viscosity.

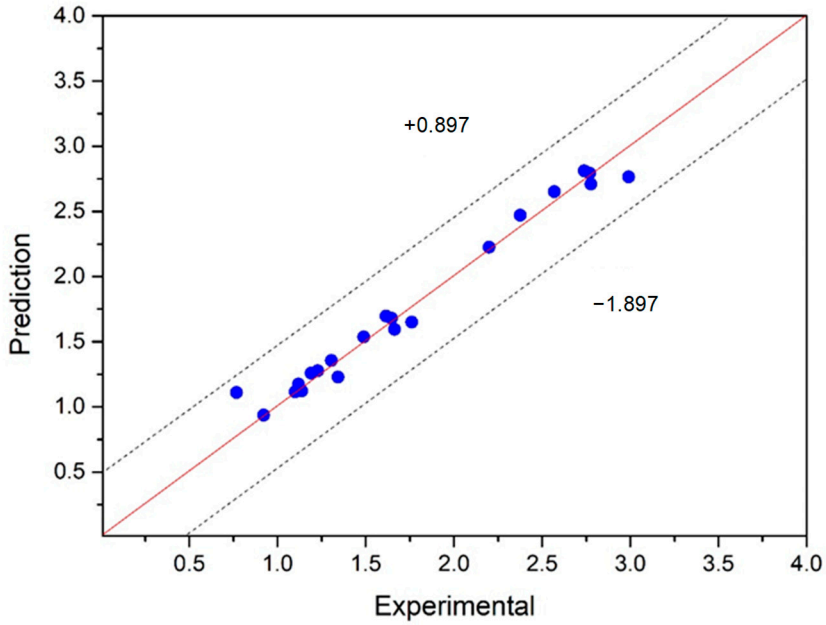

Figure 10. Comparison of the experimental and predicted model of the thermal conductivity.

3.2.5. Multi-Objective Optimization for Thermal and Physical Properties for CNC-CuO

Figure 11 illustrates an optimization analysis involving variables such as temperature, concentration, and the type of nanolubricant used. The red vertical lines represent the current levels of the input variables, with temperature set to 100 °C and concentration at 0.05%. These lines indicate specific conditions under which the system is being optimized. The dashed blue horizontal lines in the rows labeled "Thermal Minimum" and "Viscosity Minimum" represent target or minimum threshold levels that the system aims to achieve. For instance, the thermal minimum has a target of −0.3317, while the viscosity minimum target is set at 20.6258. These values indicate the desired performance levels for thermal and viscosity properties under the given conditions. Additionally, the black circles represent data points corresponding to different types of

MXene, such as CNC and CNC–MXene. These circles plot how each type of nanolubricants performs in relation to the input factors (temperature and concentration) and the target output values (thermal and viscosity minimums).

The optimum value shown in the plot is 17.0685 for dynamic viscosity and 0.3317 for thermal conductivity. The relevant parameters, such as concentration and temperature, are 30 °C and 0.01%. The composite desirability shown in the plot is 1, indicating excellent fulfillment of all criteria. Interestingly, both thermal conductivity and dynamic viscosity properties improve at lower concentrations, suggesting a synergistic effect in optimizing these parameters. Notably, there are no significant trade-offs between thermal conductivity and dynamic viscosity properties under these conditions, as both are optimized under similar circumstances. However, the steep slopes in certain areas of the response curves, particularly for dynamic viscosity, suggest that the nanolubricant performance could be sensitive to slight deviations from these optimal conditions. This optimization analysis offers valuable guidance for tailoring the CNC–MXene hybrid nanolubricant properties to specific applications, highlighting the advantages of lower temperature and concentration for improved thermal conductivity and dynamic viscosity characteristics.

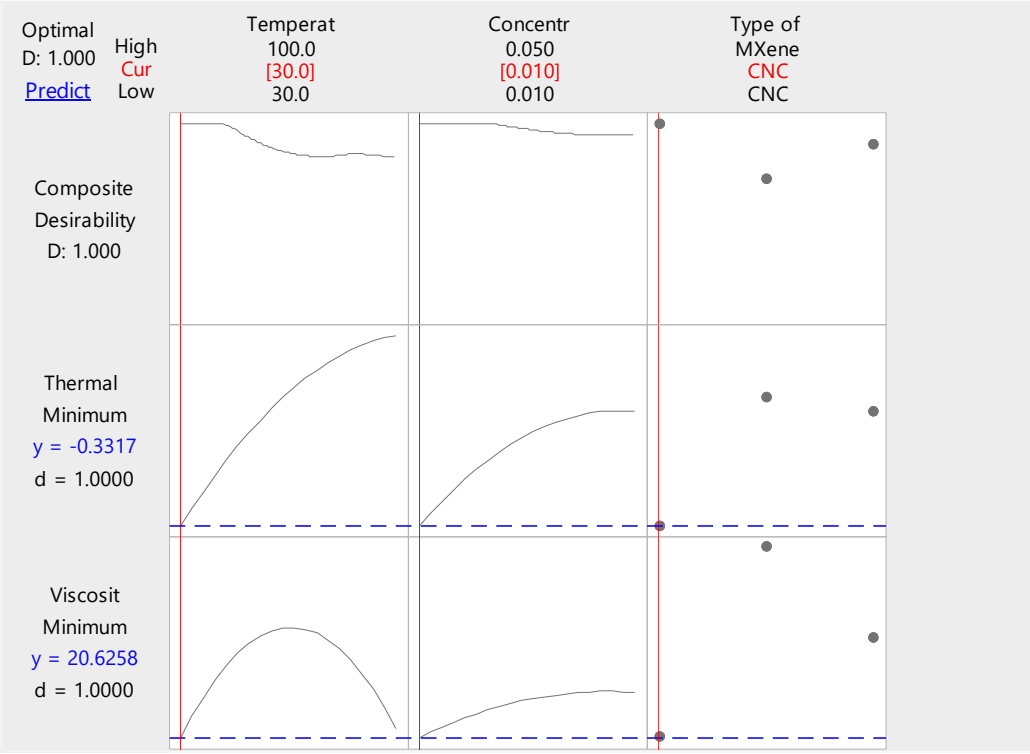

Figure 11. Optimization plot.

To validate the optimization results for the CNC–MXene hybrid nanolubricant, several steps should be taken. First, experimental validation under the optimized conditions (30 °C and 0.01% concentration of CNC) should confirm that the actual performance aligns with the predicted outcomes. A sensitivity analysis can then assess how slight variations in temperature and concentration affect performance, particularly in terms of dynamic viscosity and thermal conductivity. Comparing the optimized lubricant's performance with a standard lubricant under similar conditions will help determine if the improvements are significant. In that case, an experiment to measure thermal conductivity and dynamic viscosity was run to validate the predicted optimization results using the optimized factors. In the optimal conditions, fluid properties were measured and compared with the data predicted by the model. As shown

in Table 7, the results indicate that the model can predict the optimal experimental conditions well.

Table 7. Optimal condition values for thermophysical properties.

Optimum Results	Temperature	Concentration	Experimental Value	Predicted Value	POAE%
Dynamic viscosity	30	0.01%	22.4621	20.6258	8.902%
Thermal	30	0.01%	0.3156	0.3317	4.853%

4. Conclusions

This study has successfully investigated the synthesis, characterization, and optimization of hybrid CNC–MXene nanolubricants, providing valuable insights into their thermophysical properties and potential applications in tribological systems. The key findings and implications of this research are summarized as follows:

1. FTIR and TGA analyses confirmed the successful integration of flake MXene nanoparticles with fibrous CNC, demonstrating the feasibility of combining these materials in a nanolubricant formulation.
2. The application of Response Surface Methodology (RSM) based on Central Composite Design (CCD) yielded robust empirical mathematical models for predicting the thermophysical properties of the nanolubricants. These models demonstrated high accuracy, accounting for more than 85% of the output variations and thus providing a reliable tool for property prediction and optimization.
3. The study also revealed complex relationships between temperature, concentration, and the resulting dynamic viscosity and thermal conductivity of the nanolubricants. The non-linear behavior observed, particularly in the viscosity response to temperature changes, highlights the importance of careful optimization for specific application conditions.
4. The optimization analysis identified optimal conditions for maximizing both dynamic viscosity and thermal conductivity. The predicted optimal values (17.0685 for dynamic viscosity and 0.3317 for thermal conductivity) were achieved at 30 °C and a 0.01% concentration, with a composite desirability of 0.6531. This demonstrates the potential for tailoring nanolubricant properties to meet specific performance requirements.
5. The low percentage of absolute error (POAE) in predicting optimum experimental parameters underscores the reliability and practical applicability of the developed models. This validation enhances confidence in using these models for future nanolubricant formulation and optimization efforts.
6. The incorporation of bio-derived CNC in the hybrid nanolubricant aligns with growing sustainability efforts in industrial lubricant development, potentially offering a more environmentally friendly alternative to conventional options.

Author Contributions: Conceptualization, K.K.; formal analysis, L.S. and N.A.; investigation, N.S.; methodology, S.H. and M.K.K.; writing—original draft, S.H. and K.K.; writing—review and editing, D.R. and C.K.K. All authors have read and agreed to the published version of the manuscript.

Funding: The authors thank the Ministry of Higher Education (RDU240121**)** for providing financial support. Sakinah binti Muhamad Hisham is the recipient of the UMP Post-Doctoral Fellowship in Research.

Data Availability Statement: The data will be made available on request.

Conflicts of Interest: The authors declare no conflicts of interest.

References

1. Uniyal, P.; Gaur, P.; Yadav, J.; Khan, T.; Ahmed, O.S. A Review on the Effect of Metal Oxide Nanoparticles on Tribological Properties of Biolubricants. *ACS Omega* **2024**, *9*, 12436–12456.
2. Kamarulzaman, M.K.; Hisham, S.; Kadirgama, K.; Ramasamy, D.; Samykano, M.; Said, Z.; Pandey, A. Improvement in stability and thermophysical properties of CNC-MXene nanolubricant for Tribology application. *J. Mol. Liq.* **2023**, *381*, 121695.
3. Korkmaz, M.E.; Gupta, M.; Ross, N.S.; Sivalingam, V. Implementation of green cooling/lubrication strategies in metal cutting industries: A state of the art towards sustainable future and challenges. *Sustain. Mater. Technol.* **2023**, *36*, e00641.
4. Hisham, S.; Kadirgama, K.; Alotaibi, J.G.; Alajmi, A.E.; Ramasamy, D.; Sazali, N.; Kamarulzaman, M.K.; Yusaf, T.; Samylingam, L.; Aslfattahi, N. Enhancing stability and tribological applications using hybrid nanocellulose-copper (II) oxide (CNC-CuO) nanolubricant: An approach towards environmental sustainability. *Tribol. Int.* **2024**, *194*, 109506.
5. Shojaeiarani, J.; Bajwa, D.S.; Chanda, S. Cellulose nanocrystal based composites: A review. *Compos. Part C Open Access* **2021**, *5*, 100164.
6. Jiang, X.; Kuklin, A.V.; Baev, A.; Ge, Y.; Ågren, H.; Zhang, H.; Prasad, P.N. Two-dimensional MXenes: From morphological to optical, electric, and magnetic properties and applications. *Phys. Rep.* **2020**, *848*, 1–58.
7. Said, Z.; Rahman, S.; Assad, M.E.H.; Alami, A.H. Heat transfer enhancement and life cycle analysis of a Shell-and-Tube Heat Exchanger using stable CuO/water nanofluid. *Sustain. Energy Technol. Assess.* **2019**, *31*, 306–317.
8. Habibi, H.; Zoghi, M.; Chitsaz, A.; Javaherdeh, K.; Ayazpour, M. Thermo-economic performance comparison of two configurations of combined steam and organic Rankine cycle with steam Rankine cycle driven by Al_2O_3-therminol VP-1 based PTSC. *Sol. Energy* **2019**, *180*, 116–132.
9. Mousavi, S.B.; Heyhat, M.M. Numerical study of heat transfer enhancement from a heated circular cylinder by using nanofluid and transverse oscillation. *J. Therm. Anal. Calorim.* **2019**, *135*, 935–945.
10. Mahian, O.; Kolsi, L.; Amani, M.; Estellé, P.; Ahmadi, G.; Kleinstreuer, C.; Marshall, J.S.; Siavashi, M.; Taylor, R.A.; Niazmand, H. Recent advances in modeling and simulation of nanofluid flows-Part I: Fundamentals and theory. *Phys. Rep.* **2019**, *790*, 1–48.
11. Ahmed, S.; Ara, G.; Susan, M.A.B.H. Green Nanomaterials for Photocatalytic Degradation of Toxic Organic Compounds. *Curr. Pharm. Biotechnol.* **2023**, *24*, 118–144.
12. Wang, Q.; Zhu, T.; Li, Z.; Zhu, X.; Liu, J.; Sun, B. Plasma activation of methane for hydrogen in microwave liquid discharge by auxiliary gases: A way to realize efficient utilization of resources. *Fuel* **2022**, *330*, 125673.
13. Patel, R.K.; Sabar, S.K.; Ghosh, S.K. The heating effect on tribological behaviour in the hot rolling process using TiO_2 oil-in-water emulsion-A comparative study. *Powder Technol.* **2024**, *432*, 119112.
14. Arjmandi, H.; Amiri, P.; Pour, M.S. Geometric optimization of a double pipe heat exchanger with combined vortex generator and twisted tape: A CFD and response surface methodology (RSM) study. *Therm. Sci. Eng. Prog.* **2020**, *18*, 100514.
15. Paw, J.K.S.; Kiong, T.S.; Kamarulzaman, M.K.; Adam, A.; Hisham, S.; Kadirgama, K.; Ramasamy, D.; Yaw, C.T.; Yusop, A.F.; Yusaf, T. Advancing renewable fuel integration: A comprehensive response surface methodology approach for internal combustion engine performance and emissions optimization. *Heliyon* **2023**, *9*, e22238.
16. Nasirzadehroshenin, F.; Maddah, H.; Sakhaeinia, H. Experimental and theoretical investigation of thermophysical properties of synthesized hybrid nanofluid developed by modeling approaches. *Arab. J. Sci. Eng.* **2020**, *45*, 7205–7218.
17. Peng, Y.; Khaled, U.; Al-Rashed, A.A.; Meer, R.; Goodarzi, M.; Sarafraz, M. Potential application of Response Surface Methodology (RSM) for the prediction and optimization of thermal conductivity of aqueous CuO (II) nanofluid: A statistical approach and experimental validation. *Phys. A Stat. Mech. Its Appl.* **2020**, *554*, 124353.
18. Eastman, J.A.; Choi, S.; Li, S.; Yu, W.; Thompson, L. Anomalously increased effective thermal conductivities of ethylene glycol-based nanofluids containing copper nanoparticles. *Appl. Phys. Lett.* **2001**, *78*, 718–720.
19. Mariano, A.; Pastoriza-Gallego, M.J.; Lugo, L.; Mussari, L.; Piñeiro, M.M. Co_3O_4 ethylene glycol-based nanofluids: Thermal conductivity, viscosity and high pressure density. *Int. J. Heat Mass Transf.* **2015**, *85*, 54–60.
20. Sezer, N.; Atieh, M.A.; Koç, M. A comprehensive review on synthesis, stability, thermophysical properties, and characterization of nanofluids. *Powder Technol.* **2019**, *344*, 404–431. https://doi.org/10.1016/j.powtec.2018.12.016.
21. Zhu, D.; Li, X.; Wang, N.; Wang, X.; Gao, J.; Li, H. Dispersion behavior and thermal conductivity characteristics of Al_2O_3–H_2O nanofluids. *Curr. Appl. Phys.* **2009**, *9*, 131–139.
22. Khormali, A.; Ahmadi, S. Experimental and modeling analysis on the performance of 2-mercaptobenzimidazole corrosion inhibitor in hydrochloric acid solution during acidizing in the petroleum industry. *J. Pet. Explor. Prod. Technol.* **2023**, *13*, 2217–2235.
23. Ghafari, S.; Aziz, H.A.; Isa, M.H.; Zinatizadeh, A.A. Application of response surface methodology (RSM) to optimize coagulation–flocculation treatment of leachate using poly-aluminum chloride (PAC) and alum. *J. Hazard. Mater.* **2009**, *163*, 650–656.
24. Kumar, B.R.; Saravanan, S.; Rana, D.; Nagendran, A. Combined effect of injection timing and exhaust gas recirculation (EGR) on performance and emissions of a DI diesel engine fuelled with next-generation advanced biofuel–diesel blends using response surface methodology. *Energy Convers. Manag.* **2016**, *123*, 470–486.
25. Wang, B.; Wang, H.; Tu, B.; Zheng, K.; Gu, H.; Wang, W.; Fu, Z. Optical transmission, dispersion, and transition behavior of $ZnGa_2O_4$ transparent ceramic. *J. Am. Ceram. Soc.* **2023**, *106*, 1230–1239.
26. Dhanola, A.; Gajrani, K.K. Novel insights into graphene-based sustainable liquid lubricant additives: A comprehensive review. *J. Mol. Liq.* **2023**, 122523.

27. Mohammadi, M.; Dadvar, M.; Dabir, B. TiO_2/SiO_2 nanofluids as novel inhibitors for the stability of asphaltene particles in crude oil: Mechanistic understanding, screening, modeling, and optimization. *J. Mol. Liq.* **2017**, *238*, 326–340.
28. Kumar, R.; Antonov, M. Self-lubricating materials for extreme temperature tribo-applications. *Mater. Today Proc.* **2021**, *44*, 4583–4589. https://doi.org/10.1016/j.matpr.2020.10.824.
29. Rostamian, H.; Lotfollahi, M.N. A novel statistical approach for prediction of thermal conductivity of CO_2 by Response Surface Methodology. *Phys. A Stat. Mech. Its Appl.* **2019**, *527*, 121175.
30. Rostamian, H.; Lotfollahi, M.N. New functionality for energy parameter of Redlich-Kwong equation of state for density calculation of pure carbon dioxide and ethane in liquid, vapor and supercritical phases. *Period. Polytech. Chem. Eng.* **2016**, *60*, 93–97.
31. Esfe, M.H.; Firouzi, M.; Rostamian, H.; Afrand, M. Prediction and optimization of thermophysical properties of stabilized Al2O3/antifreeze nanofluids using response surface methodology. *J. Mol. Liq.* **2018**, *261*, 14–20.
32. Borode, A.; Olubambi, P. Modelling the effects of mixing ratio and temperature on the thermal conductivity of GNP-Alumina hybrid nanofluids: A comparison of ANN, RSM, and linear regression methods. *Heliyon* **2023**, *9*, e19228.

Disclaimer/Publisher's Note: The statements, opinions and data contained in all publications are solely those of the individual author(s) and contributor(s) and not of MDPI and/or the editor(s). MDPI and/or the editor(s) disclaim responsibility for any injury to people or property resulting from any ideas, methods, instructions or products referred to in the content.